AD-A126 444 FURTHER STUDIES ON DYNAMIC CRACK BRANCHING(U) 1/1
WASHINGTON UNIV SEATTLE DEPT OF MECHANICAL ENGINEERING
M RAMULU ET AL. MAR 83 UWA/DME/TR-82/46
UNCLASSIFIED N00014-76-C-0060 F/G 20/11 NL

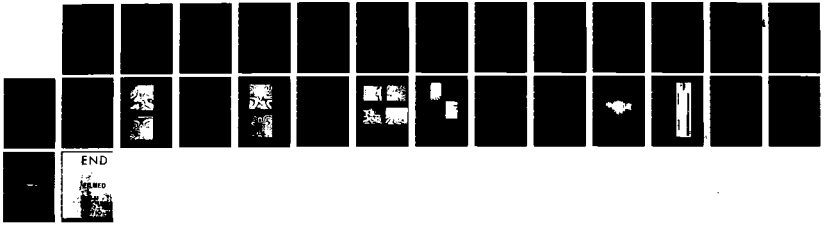

END

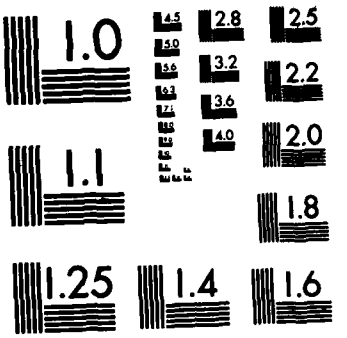

(12)

Office of Naval Research

Contract N00014-76-0060 NR 064-478

Technical Report No. UWA/DME/TR-82/46

FURTHER STUDIES ON DYNAMIC CRACK BRANCHING

by

M. Ramulu, A. S. Kobayashi, B. S.-J. Kang and D. B. Barker

March 1983

The research reported in this technical report was made possible through support extended to the Department of Mechanical Engineering, University of Washington, by the Office of Naval Research under Contract N00014-76-C-0060 NR 064-478. Reproduction in whole or in part is permitted for any purpose of the United States Government.

Department of Mechanical Engineering

College of Engineering

University of Washington

FURTHER STUDIES ON DYNAMIC CRACK BRANCHING

by

M. Ramulu,* A. S. Kobayashi,* B. S.-J. Kang,* and D. B. Barker**

ABSTRACT

The newly derived dynamic crack branching criterion is verified by dynamic photoelastic analysis of dynamic crack branchings in thin polycarbonate, single edged crack tension specimens. Successful crack branching was observed in four specimens and unsuccessful branchings in another. Crack branching consistently occurred when the necessary condition of K_{Ib} = 3.3 MPa $m\sqrt{}$ and the sufficient condition of $r_o = r_c$ = 0.7 mm were satisfied simultaneously. In the unsuccessful branching test the necessary conditon was not satisfied since K_I was always less than K_{Ib}.

INTRODUCTION

Crack branching represents one extreme of the large range of dynamic crack propagation behaviors and has been the subject of numerous theoretical and experimental investigations, several of which can be found in References [1,2]. Recently, the authors derived a crack curving and a branching criteria based on the directional stability of a propagating crack [3,4]. The crack

---

* Research Assistant Professor, Professor and Graduate Student, respectively, University of Washington, Department of Mechanical Engineering, Seattle, WA 98195

**Visiting Associate Professor, University of Washington, Department of Mechanical Engineering at the time of this writing.

curving criteria is a micro-mechanical model of continuous micro-flaw growth and coalescence in the vicinity of the moving crack tip. It assumes that the crack is momentarily kinked or bifurcated, when an off-axis micro-flaw connects with the crack tip and is the dynamic extension of the crack curving criterion proposed by Streit and Finnie [5].

The dynamic crack curving criterion has been used to predict the crack kinking angle of a propagating crack under pure mode I as well as mixed mode condtions[3]. The crack branching criterion on the other hand, requires a critical stress intensity factor to trigger crack branching and a crack curving criterion for predicting the crack branching angle [4,6]. The objective of this paper is to provide further evidence in support of the dynamic crack branching criterion advanced by the authors.

CRACK BRANCHING CRITERION

The crack branching criterion [6] requires, as the sufficiency condition, a crack curving criterion [4]. The latter is based on the postulate that the micro-cracks ahead of the crack tip dictate the direction of crack propagation. When an off-axis, i.e., $\theta \neq 0$, micro-void, which is within a critical distance, r_c, to the crack tip, is actuated by a critical crack tip stress field, it deflects the crack from its otherewise self-similar propagation path. The distance between the micro-void and the crack tip, r_o, is a characteristic distance which is governed by the singular state of stress as well as the stress acting parallel to the crack, commonly referred to as either the remote stress or the non-singular stress component, σ_{ox}. The critical distance, r_c, is assumed to be a material property.

The angular orientation of this critical micro-void is determined by the maximum circumferential stress criterion, as modified by Ramulu and Kobayashi [3], which assumes that the crack will extend towards the maximum circumferential stress at a distance, r, away from the rapidly propagating crack tip. Based on this assumption, under pure mode I loading, i.e., $K_I^* \neq 0$, $K_{II} = 0$, the condition for self-similar propagation of a straight crack is obtained by setting $\theta = 0$ as

$$r_o = \frac{1}{128\pi}\left(\frac{K_I}{\sigma_{ox}} v_o(c, c_1, c_2)\right)^2$$

where

$$V_o(c,c_1c_2)=B_1(c)\{-(1+S_2^2)(2-3S_1^2)-\frac{4S_1S_2}{1+S_2^2}(14+3S_2^2)-16S_1(S_1S_2)+16(1+S_1^2)\}$$

$$S_1^2 = 1 - \frac{c^2}{c_1^2} \quad ; \quad S_2^2 = 1 - \frac{c^2}{c_2^2}$$

c = crack velocity, m/s

c_1 = dilatational wave velocity, m/s

c_2 = distortional wave velocity, m/s

Here, K_I, σ_{ox} and r_o, are the mode I stress intensity factor, remote stress and the characteristic distance, respectively, and can be determined from the current dynamic state of stress. The onset of crack curving of a rapidly propagating crack is governed by the stability of the propagating straight crack and is assumed to occur when $r_o \leq r_c$. This r_c is a characteristic distance derived from a directional stability criterion involving the critical crack tip state of stress where θ suddenly becomes non-zero. The corresponding angle, θ_c, for a maximum circumferential stress can be determined from a transcendental relation involving the critical values of r_c and θ_c which is derived from maximizing the off-axis maximum circumferential stress.

*The superscript "dyn" to identify dynamic stress intensity factor will not be used in this paper, since all quantitites refer to dynamic values.

The crack branching criterion, however, involves not only the critical r_c but also the maximum K_I as a necessary condition for the growth of multiple off-axis secondary cracks, and $r_o < r_c$ as a sufficiency condition for these multiple cracks to kink simultaneously. Therefore, the crack branching criterion can be stated as

$$K_I = \text{Max. } K_I = K_{Ib} \qquad \text{Necessary condition}$$

$$r_o \leq r_c \qquad \text{Sufficiency condition}$$

The crack curving angle θ_c determined from the latter crack curving criterion is one half of the included crack branching angle.

Crack Branching in Homalite-100 Fracture Specimens and Pressurized Pipes

The validity of the above crack curving and crack branching criteria was verified by dynamic photoelasticity results of Homalit-100 single edged-notch (SEN) specimens and the wedge-loaded, rectangular double-cantilever beam (WL-RDCB) specimens with branched cracks [3,4,6]. Crack branchig consistently occurred when the dynamic stress intensity factor reached a crack branching stress intensity factor $K_{Ib} = 2.04$ MPa$\sqrt{m}$ and the characteristic distance r_o was less than critical distance of $r_c = 1.3$ mm. The crack branching angles of bifurcated cracks in SEN specimens was smaller than in the WL-RDCB specimens. Differences in crack branching angles are expected since the non-singular stress, σ_{ox}, in the SEN specimens is compressive and suppresses the branching angle whereas the tensile σ_{ox} in WL-RDCB enchances the branching angle. The crack branching angles in pressurized steel of Reference [7,8] and aluminum pipes of Reference [9] were also predicted by this crack branching criterion [6].

POLYCARBONATE FRACTURE SPECIMENS

In order to further verify the dynamic crack branching criterion, a series of dynamic photoelastic fracture experiments involving thin polycarbonate fracture experiments were conducted. The single edged notch specimens with blunt starter crack were 127 x 225 mm and 3.2 mm or 6.4 mm thick. At fracture load, the crack propagated from the starter crack and branched. The dynamic isochromatics surrounding the propagating crack were recorded with a 16 spark gap Cranz-Schardin camera system.

The fracture parameters of K_I, K_{II} and σ_{ox} [10] associated with the running crack were determined by least square fitting a theoretical dynamic mixed-mode stress field to the recorded dynamic isochromatics. The isochromatic fringe loops were digitized and analyzed on a PDP-11/44 computer. A least square algorithm was used to determine K_I, K_{II} and σ_{ox} from the multi-point isochromatic data as reported in Ref. [11,12]. The estimated fracture parameters were then used to generate the corresponding theoretical isochromatics which were superposed on the experimental isochromatics for a visual evaluation of the accuracy of the fitting process. A flow chart of this on-line estimation of the dynamic fracture parameters from the recorded dynamic isochromatics is shown in Figure 1.

RESULTS

Figure 2 shows two typical dynamic isochromatic patterns in a 3.2 mm thick, fracturing polycarbonate SEN specimen. At fracture load, the crack initiated and propagated from a blunt starter crack with several unsuc-

cessful attempts at branching prior to a successful branching.

Figure 3 shows K_I, K_{II} and σ_{ox} variations associated with the crack branching experiment of Figure 2. The crack after initiation, propagated with a gradual increase in its dynamic stress intensity factor. Immediately prior to branching, the instantaneous dynamic stress intensity factor reached its maximum value of 3.3 MPa$\sqrt{m}$ with negligible K_{II} and the associated remote stress, σ_{ox}, attained a value of 11.2 MPa. By smoothly extrapolating the average K_I and K_{II} associated with the two branch cracks, an after-branching $K_I \doteq 2.2$ MPa$\sqrt{m}$ and $K_{II} \doteq \pm 0.9$ MPa$\sqrt{m}$ are obtained.

Figure 4 shows two frames of the 16-frame dynamic photoelastic record of a propagating and branching crack in a 3.2 mm thick, polycarbonate SEN specimen. The crack emanated from a blunt saw cut crack and propagated through much of the length of the plate with innumerable unsuccessful branching prior to the successful crack branching. Note that post-arrest isochromatics surrounding all unsuccessful branches exhibit a pure mode II crack tip deformation.

Figure 5 shows the dynamic K_I, K_{II} and σ_{ox} variations obtained from the photoelastic patterns preceding and after crack branching from the test shown in Figure 4. Immediately prior to the crack branching, the extrapolated values of K_I and σ_{ox} at the onset of crack branching yielded a branching stress intensity factor of $K_I = 3.3$ MPa$\sqrt{m}$. σ_{ox} had gradually reached a value of 11.5 MPa, which is consistent with previous test results. Immediately after branching, extrapolated after-branching the average Mode I and Mode II stress intensity factors of $K_I \doteq 2.2$ MPa$\sqrt{m}$ and $K_{II} \doteq \pm 0.9$ MPa$\sqrt{m}$ were obtained.

Figure 6 shows four frames out of a 16-frame dynamic photoelastic record of another test with multiple crack branching. Although no attempt was made to analyze these post-branched multiple cracks, the data up to the onset of successful crack branching yielded again $K_1 = K_{Ib} = 3.32$ MPa$\sqrt{m}$ and $\sigma_{ox} = 11.72$ MPa.

During the last ten plus years of dynamic crack branching study, we have observed that either the unsuccessfully branched cracks or the completely arrested cracks were under a pure mode II state. In the tests shown, the pure mode II isochromatics were also seen (Figures 2,4,6) at the unsuccessful branched cracks. Figure 7 shows two enlarged views of Test No. KB-8208024 of Figure 5 with a mixed-mode isochromatic pattern arres of the branched crack. Immediately after arrest the crack tip isochromatics transformed into mode II isochromatics with the 45 μ second interval. The mode I and mode II stress intensity factors K_I, K_{II} and σ_{ox} prior to and after the crack arrest are: K_I = 1.36 MPa$\sqrt{m}$, K_{II} = 0.06 MPa$\sqrt{m}$, σ_{ox} = -7.7 MPa and K_I = 0.05 MPa$\sqrt{m}$, K_{II} = 0.7 MPa m, σ_{ox} = 8.06 MPa respectively. This suggests that the arrested branch crack undergoes a mode II crack tip deformation during its unloading loading process.

Figure 8 shows the variations of K_I, K_{II} and σ_{ox} associated with a straight crack with unsuccessful branches in 3.2 mm thick specimen. Although many attempts of branchign were observed, complete branching did not occur in this specimen since the dynamic stress intensity factor was always less than the $K_{Ib} = 3.3$ MPa$\sqrt{m}$. Evaluations of two additional tests yielded the crack branching data shown in Table 1. The critical values of r_c ranged from 0.6 to

0.8 mm.

The crack velocity in the five tests were essentially constant and at about 23 percent of the dilatational wave velocity, c_1 = 1955 mps. The same velocity was observed in the crack curving experiments conducted with this material [13]. It appears that this crack velocity is the maximum observed in all the dynamic fracture tests involving polycarbonate.

Figure 9 shows the variations in characteristic distance r_o, which was computed by Equation (1), for the propagating cracks prior to the crack branching in the five tests. Although the value of r_o has a scatterband of 0.5 to 0.9 mm, as shown in Figure 8, all extrapolated r_o at crack branching reached an average minimum value of 0.7 mm. This crack branching $r_o = r_c$ = 0.7 mm represents the sufficiency condition for crack curving and is consistent with the r_c value determined from the crack curving experiments of polycarbonate material [13].

Table 1 shows the crack branching stress intensity factors, K_{Ib}, the critical distance, r_c, and the measured and predicted crack branching angles of all four test results of successful crack branchings. The dynamic stress intensity factor at the onset of crack branching reached an average maximum value of 3.3 $MPa\sqrt{m}$. This branching stress intensity factor was found to be independent of the thickness of the specimen as well as the initial and branching crack lengths.

Crack branching angles were computed by using the crack curving criterion and are listed in Table 1. The average crack branching angle is 25^{o}. The branching angle in this series of SEN specimens varied between 22^{o} and 34^{o} and is consistent with our previous results involving Homalite-100 [4].

DISCUSSION

Post-branching cracks in all tests always curved. Kalthoff [14], observed that the direction of two branched cracks attraction or repulsion, is controlled by K_{II}/K_{I}. The photoelastic patterns of running branched cracks showed that the crack was perpendicular to the load direction. This strongly suggests that the crack runs parallel to the compressive stress direction even under mixed mode conditions which exist after branching. Therefore post-branching crack propagation is also strongly dependent on the K_{II}/K_{I} ratio as well as on σ_{ox}. Figure 10 shows the post-branching crack curving of specimen No. 820822. The measured and calculated angles are marked on Figure 10 show that the crack curving angle gradually decreased in magnitude along with increase in negative σ_{ox} and is in agreement with the numerical results of Ref. [15].

Figure 11 shows the typical fracture surface in a 6.4 mm thick polycarbonate SEN specimen associated with the crack branching. Clear mirror, mist and hackle zones are visible. This fractured surface indicates that the σ_{ox} term which is the parallel stress in this specimen, is compressive and opens the micro-cracks in the form of tongues. Although the dynamic stress intensoity factor is almost equal to K_{Ib}, the crack did not branch at the fine hackle zone but branched when this hackle zone became rougher and when the sufficiency condition was met.

CONCLUSIONS

1. Dynamic crack branching criterion proposed by the authors successfully predicted the crack branching when the necessary condition of $K_I = K_{Ib}$ which triggered the generation of secondary cracks, and the sufficiency condition of $r_o < r_c$, which caused the crack tip diversion, were satisfied.

2. A crack branching stress intensity factor of $K_{Ib} = 3.3$ MPa$\sqrt{m}$ and characteristic radius of $r_c = 0.7$mm are determined for this polycarbonate sheet.

3. Crack curving of post-branched cracks, attraction and repulsion, depends not only on K_{II}/K_I but more importantly on σ_{ox}. Negative σ_{ox} suppresses the crack curving irrespective of the sign of K_{II}/K_I.

ACKNOWLEDGEMENT

The work reported here was obtained under ONR Contract NO-0014-76-C-000 NR-064-478. The authors wish to acknowledge the support and encouragement of Dr. Y. Rajapakse, ONR, during the course of this investigation.

REFERENCES

1. Rossmanith, H. P., "Crack Branching of Brittle Materials, Part I", University of Maryland Report. 1977-1980.

2. Dally. J. W., "Dynamic Photoelastic Studies of Experimental Mechanics, Vol. 19, No. 10, 1979, pp. 349-367.

3. Ramulu, M. and Kobayashi, A. S., "Dynamic Crack Curving - A Photoelastic Evaluation", to be published in Experimental Mechanics.

4. Ramulu, M., Kobayashi, A. S. and Kang, B. S. J., "Dynamic Crack Branching - A Photoelastic Evaluation", to be published in Fracture Mechanics (15th), ASTM STP, 1983.

5. Streit, R. and Finnie, I., "An Experimental Investigation of Crack Path Directional Stability", Experimental Mechanics, 20, Jan. 1980, pp.17-23.

6. Ramulu, M., Kobayashi, A. S. and Kang, B. S. J., "Dyanmic Crack Curving and Branching in Line-Pipe", ASME J. of Pressure Vessel Technology, 104, Nov. 1983, pp. 317-322.

7. Almond, E. A., Petch, N. J., Wraith, A. E. and Wright, E. S., "The Fracture of Pressurized Laminated Cylinders", J. of Iron and Steel Institute, 207, October 1969, pp. 1319-1323.

8. Congleton, J., "Practical Applications of Crack-Branching Measurements", Dynamic Crack Propagation, ed. by G. C. Sih, Noordhoff Int. Pub., Leyden, 1973, pp. 427-438.

9. Shannon, R. W. E. and Wells, A. S., "A Study of Ductile Crack Propagation in Gas Pressurized Pipeline", Proc. of Int. Symp. on Pipeline, Paper No. 17, Newcastle upon Tyne, Mar. 1974.

10. Freund, L. B., "Dynamic Crack Propagation", Mechanics of Fracture, Vol. 19, ed. by F. Erdogan, ASME, 1976, pp. 105-134.

11. Kobayashi, A. S., Ramulu, M., "Dynamic Stress Intensity Factor for Unsymmetric Dynamic Isochromatics", Experimental Mechanics, Vol. 21, No. 1, 1981, pp. 41-48.

12. Sanford, R. J. and Dally, J. W., "A General Method for Determining Mixed Mode Stress Intensity Factors from Isochromatic Fringe Patterns", Eng. Fract. Mech., 11, 1979, pp. 621-633.

13. Sun, Y. J., Ramulu, M., Kobayashi, A. S. and Kang, B. S. J., "Further Studies on Dynamic Crack Curving", Developments in Theoretical and Applied Mechanics, eds. T. J. Chung and G. R. Karr, The University of Alabama, Huntsville, 1982, pp. 203-218.

14. Kalthoff, J. F., "On the Propagation of Bifurcated Cracks", Dynamic Crack Propagation, ed. by G. C. Sih, Noordhoff Int. Pub., 1973, pp. 449-458.

15. Ramulu, M. and Kobayashi, A. S., "Strain Energy Density Fracture Criterion in Elasto-dynamic Mixed Mode Crack Propagation" to be published in Engineering Fracture Mechanics.

TABLE I

SUMMARY OF CRACK BRANCHING DATA
IN POLYCARBONATE SINGLE EDGED NOTCH TENSION SPECIMENS

Test No.	Specimen Thickness h mm	Initial Crack Length a_o mm	Crack Length at Branching a_b mm	c/c_1	K_{Ib} MPa$\sqrt{m}$	σ_{ox} MPa	r_c mm	Branching Angle θ_c degrees Measured	Theoretical
KB-820826-1	3.2	15	86	0.22	3.3	-11.40	0.85	34	31
KB-820816-2	6.4	9	52	0.23	3.2	-11.48	0.78	22	28
KB-820822	3.2	16	65	0.23	3.3	-11.18	0.78	29	26
KB-820824	3.2	15	41	0.22	3.3	-14.72	0.58	25	26
			Average	0.23	3.3	12.2	0.73	25	28.5

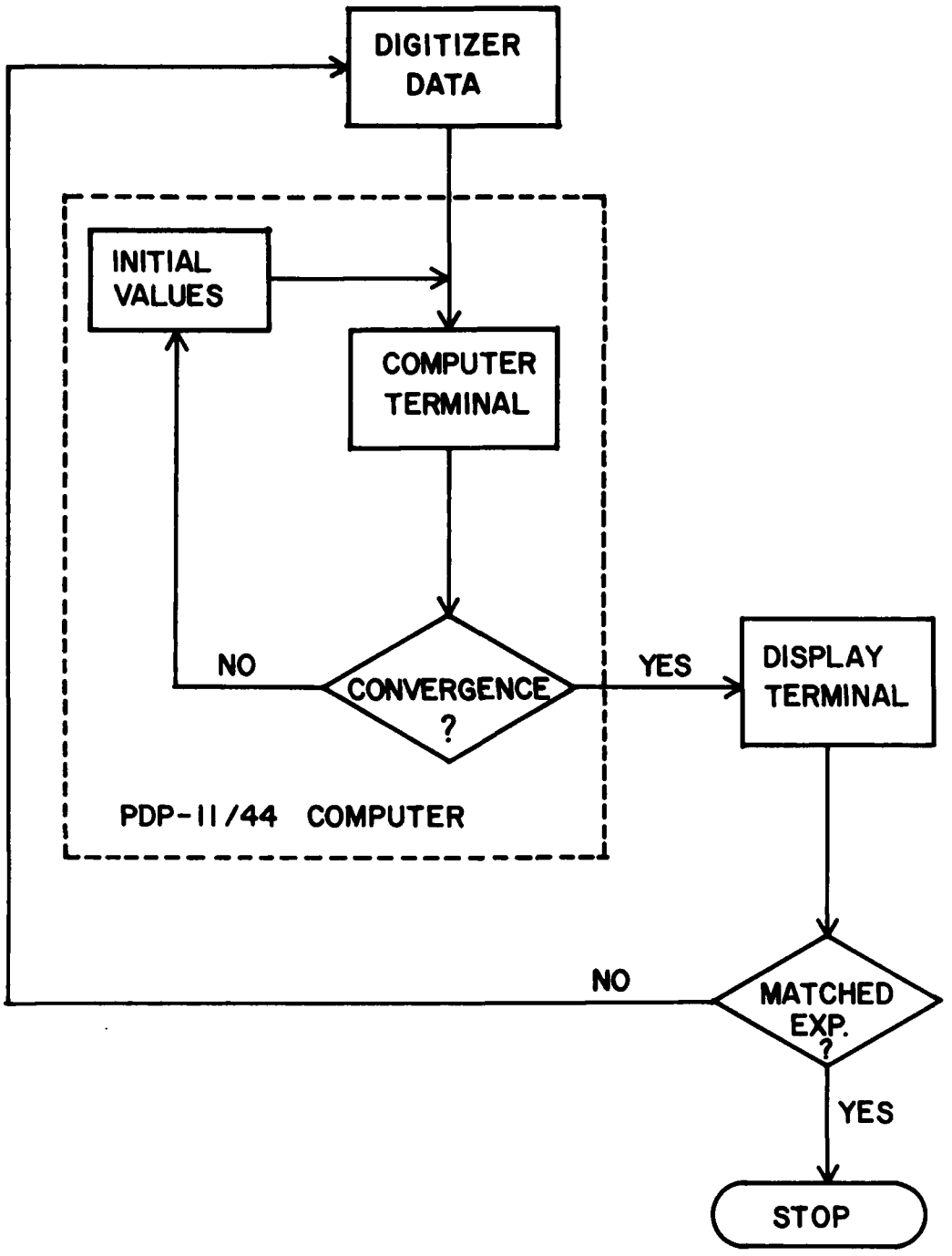

FIGURE 1. FLOW CHART FOR ON-LINE ESTIMATION OF FRACTURE PARAMETERS FROM RECORDED DYNAMIC ISOCHROMATICS

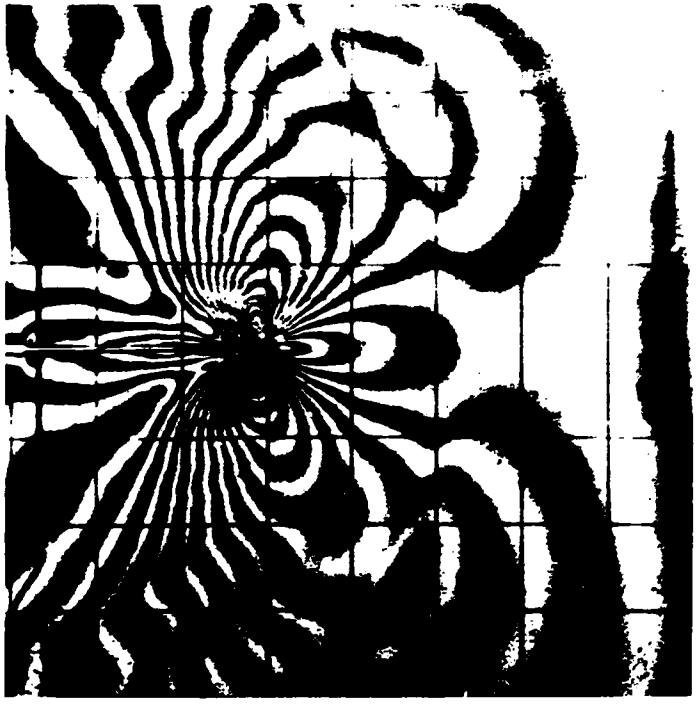

EIGHTH FRAME, 147 μ SECONDS

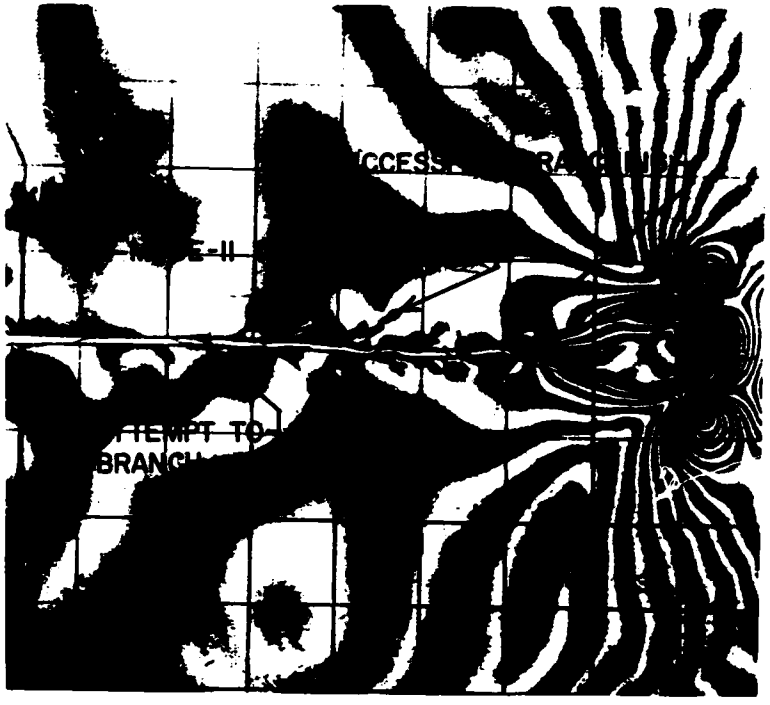

SIXTEENTH FRAME, 206 μ SECONDS

FIGURE 2. TYPICAL DYNAMIC ISOCHROMATIC PATTERNS OF CRACK BRANCHING IN A POLYCARBONATE SINGLE-EDGED NOTCH SPECIMEN. SPECIMEN NO. KB-820826-1

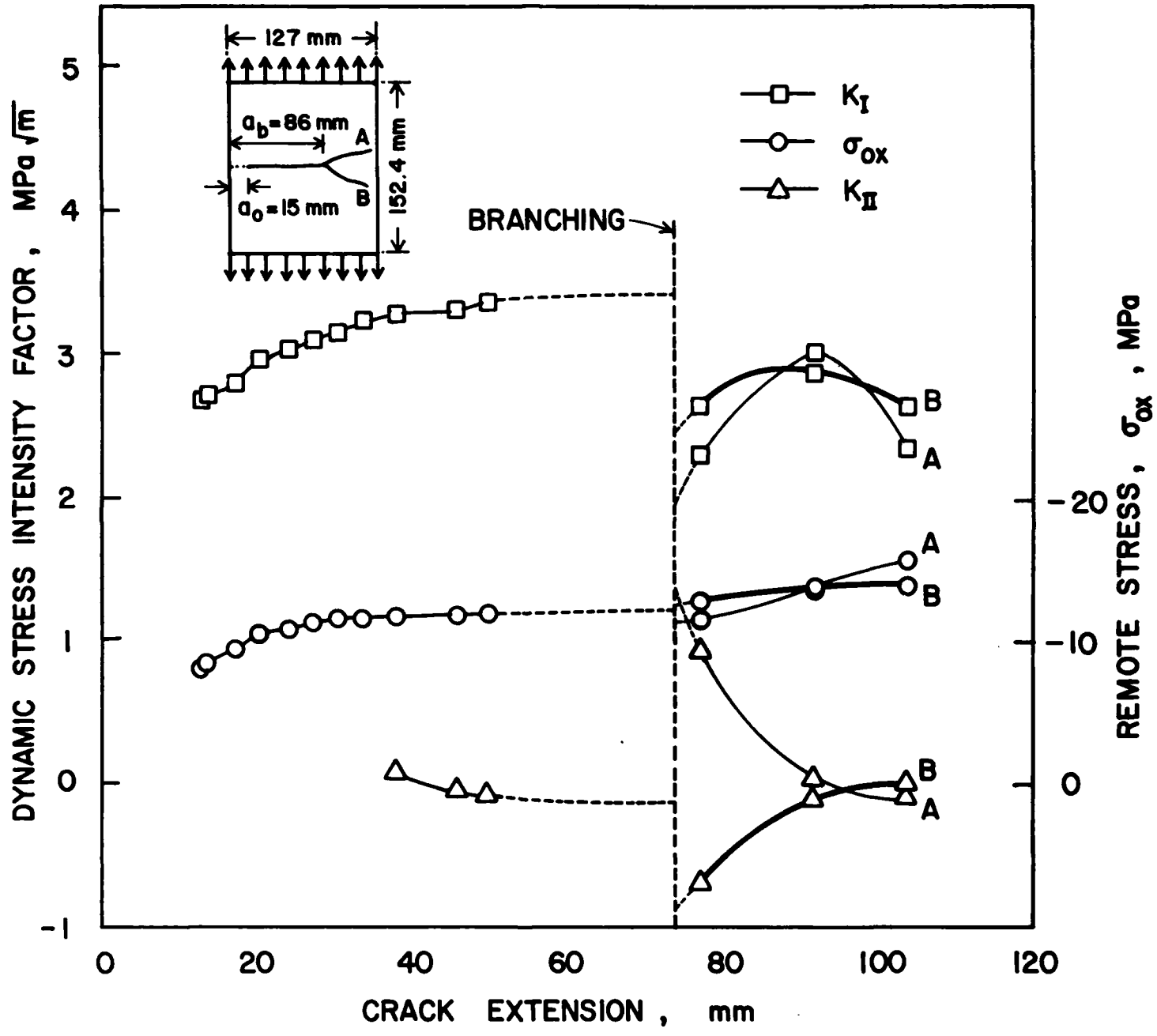

FIGURE 3. DYNAMIC STRESS INTENSITY FACTORS AND σ_{ox} OF THE BRANCHED CRACKS. SPECIMEN NO. KB-820826-1

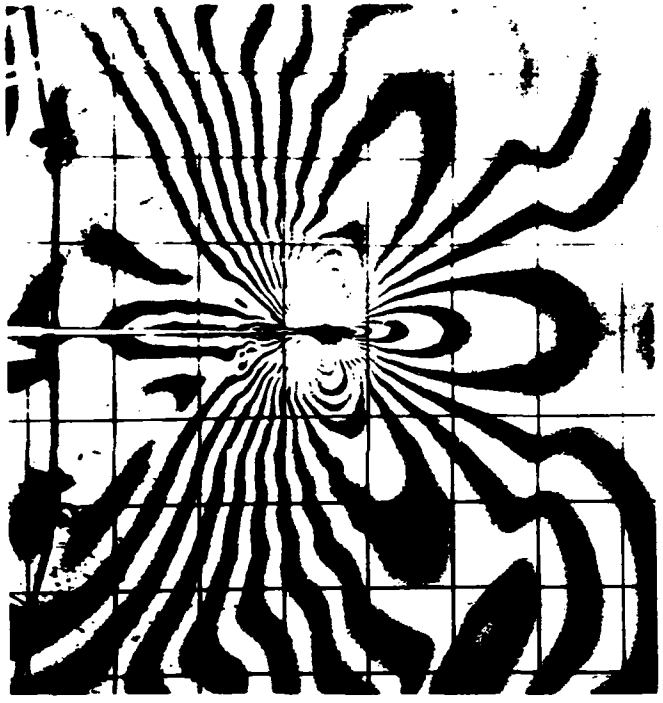

SIXTH FRAME, 59 μ SECONDS

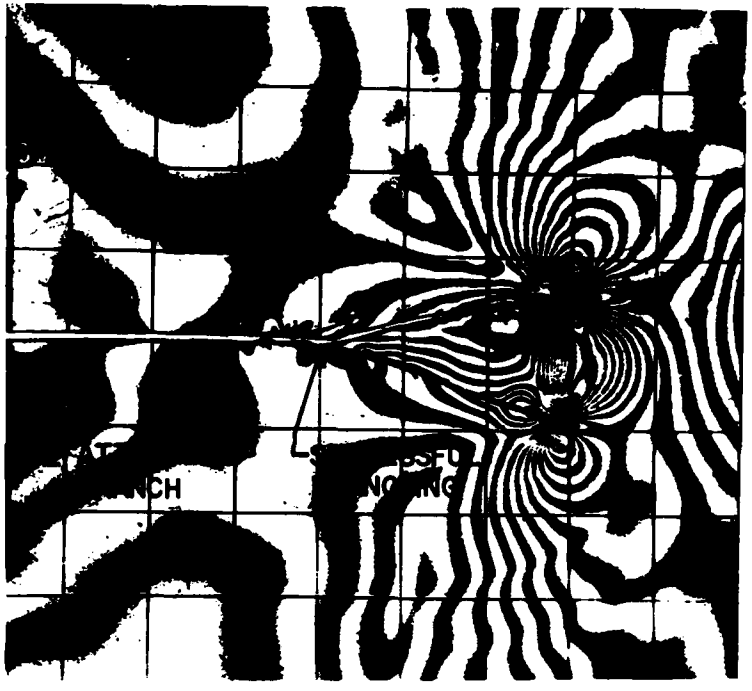

THIRTEENTH FRAME, 162 μ SECONDS

FIGURE 4. TYPICAL DYNAMIC ISOCHROMATIC PATTERNS OF CRACK BRANCHING IN A POLYCARBONATE SINGLE-EDGED NOTCH SPECIMEN. SPECIMEN NO. KB-820822

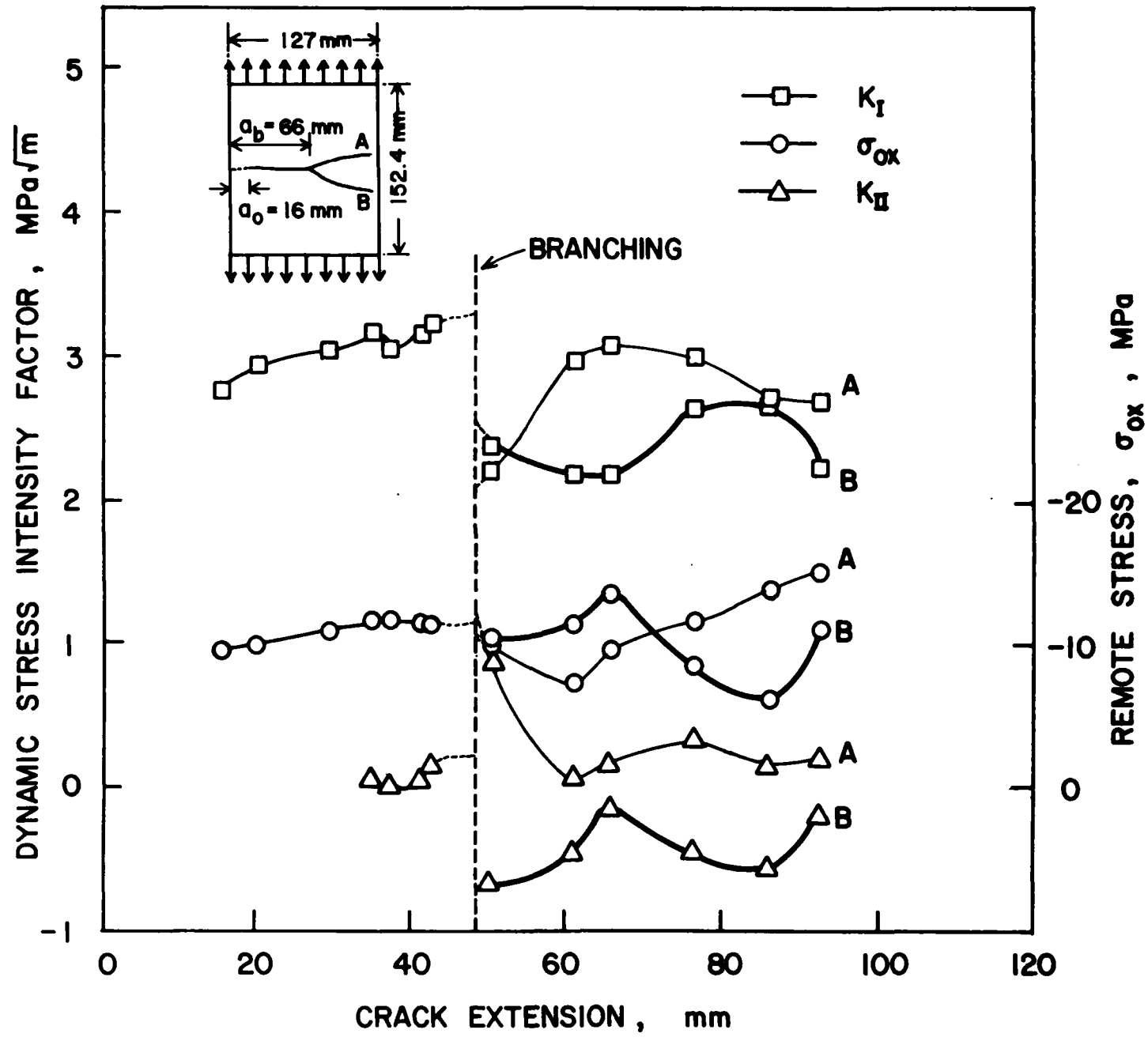

FIGURE 5. DYNAMIC STRESS INTENSITY FACTORS AND σ_{ox} OF THE BRANCHED CRACKS. SPECIMEN NO. KB-820822

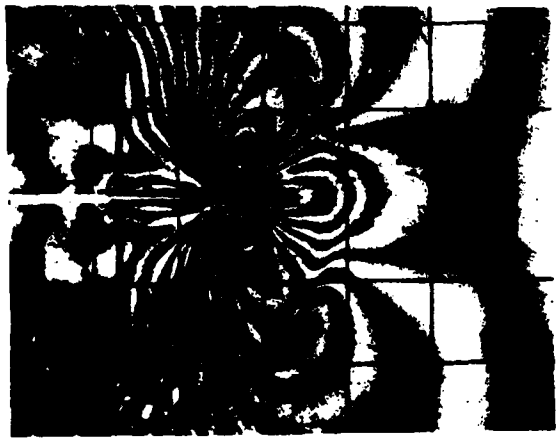

SECOND FRAME,
43 μ SECONDS

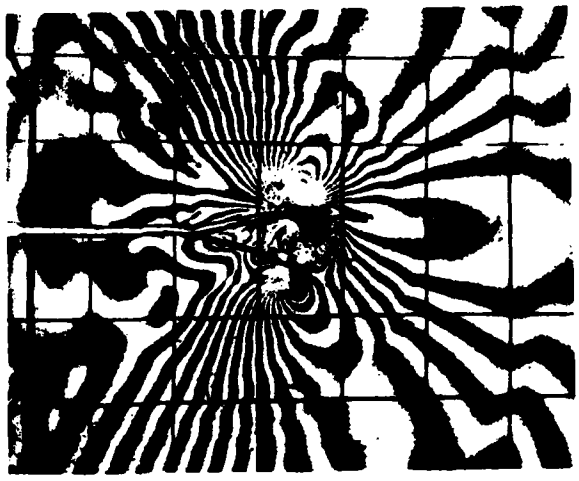

SEVENTH FRAME,
95 μ SECONDS

THIRTENTH FRAME,
176 μ SECONDS

SIXTEENTH FRAME,
262 μ SECONDS

FIGURE 6. TYPICAL DYNAMIC PHOTOELASTIC PATTERNS OF MULTIPLE CRACK BRANCHING IN A POLYCARBONATE SINGLE-EDGED NOTCH SPECIMEN.
SPECIMEN NO. KB-820824

FIFTEENTH FRAME,
217 μ SECONDS

SIXTEENTH FRAME,
262 μ SECONDS

FIGURE 7. DYNAMIC ISOCHROMATIC PATTERNS BEFORE AND AFTER CRACK ARRESTING IN BRANCHING CRACK. SPECIMEN NO. KB-820824

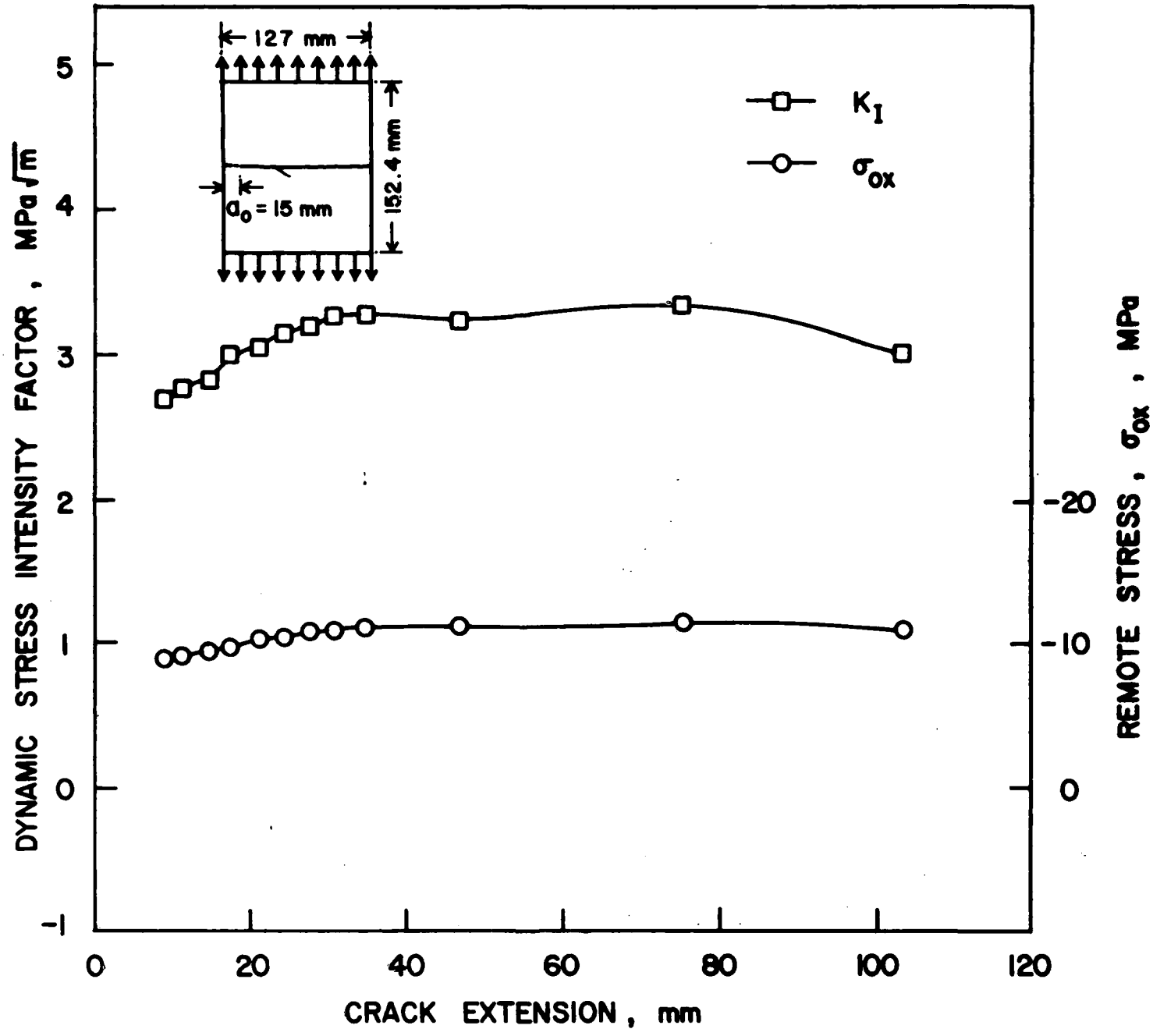

FIGURE 8. DYNAMIC STRESS INTENSITY FACTOR AND σ_{ox} OF THE

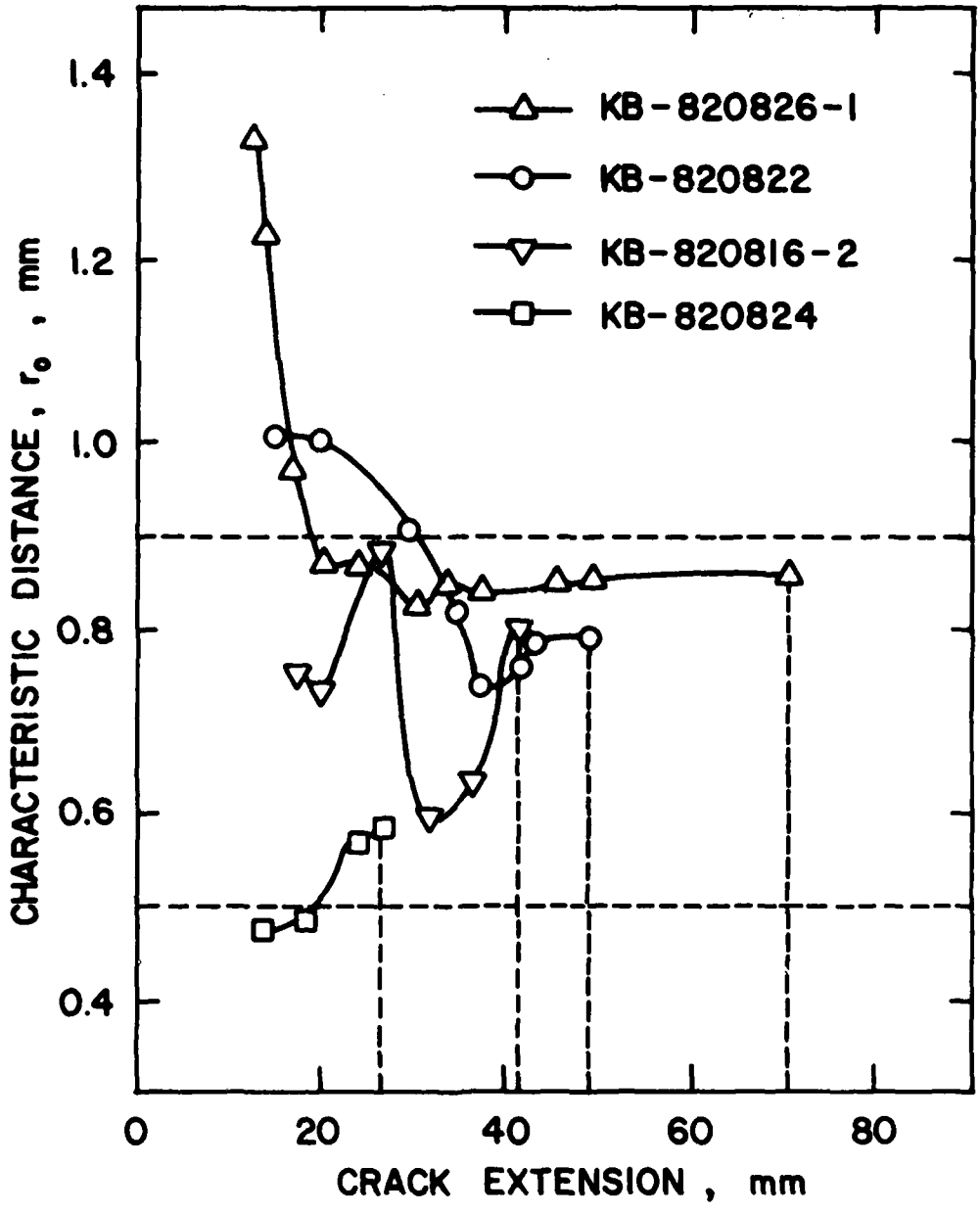

FIGURE 9. CHARACTERISTIC DISTANCE, r_o , PRIOR TO CRACK BRANCHING IN A POLYCARBONATE SINGLE EDGED NOTCH TENSION SPECIMENS.

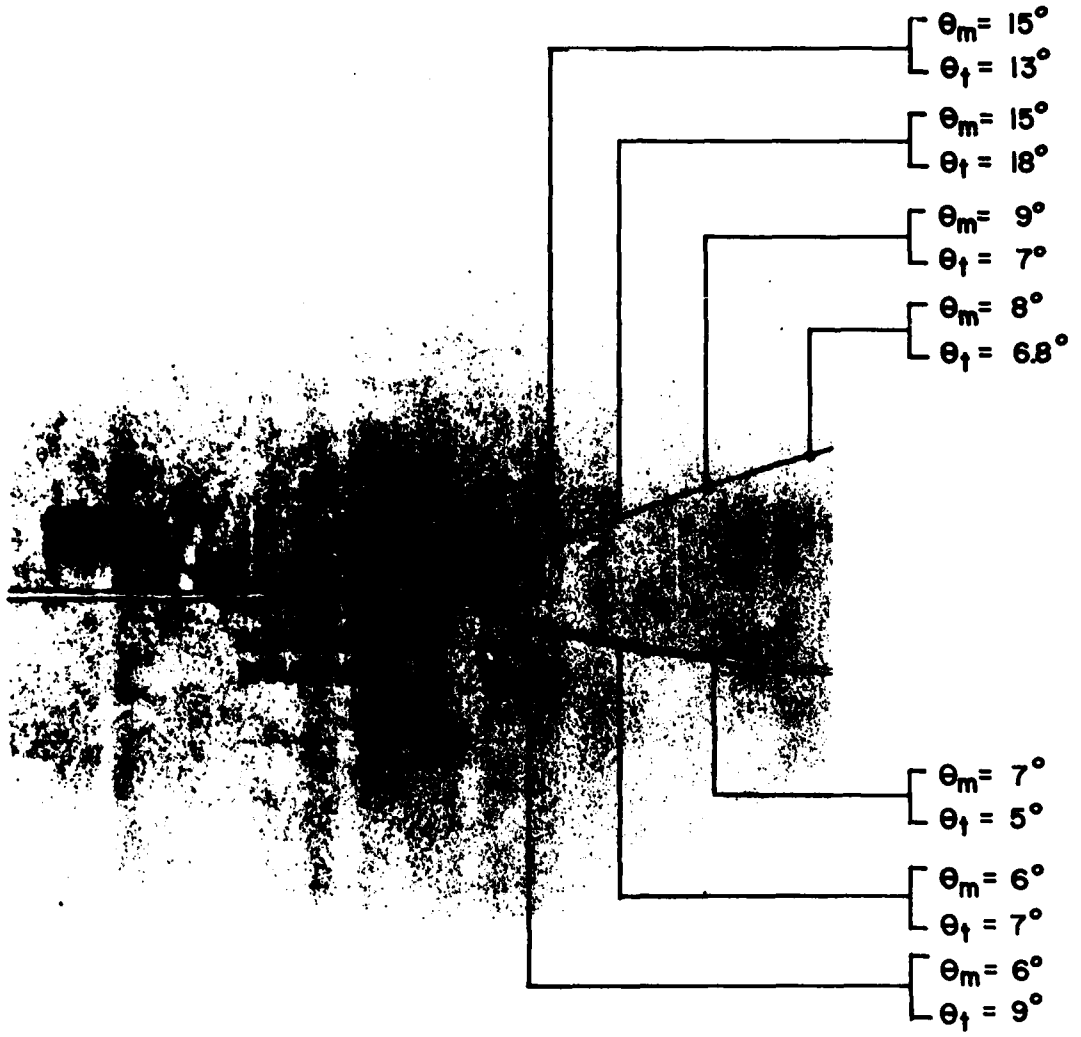

θ_m = MEASURED ANGLE

θ_t = THEORETICAL ANGLE

FIGURE 10. INCIPIENT CRACK BRANCHING AND POST BRANCHING CRACK CURVING OF SPECIMEN NO. 820822

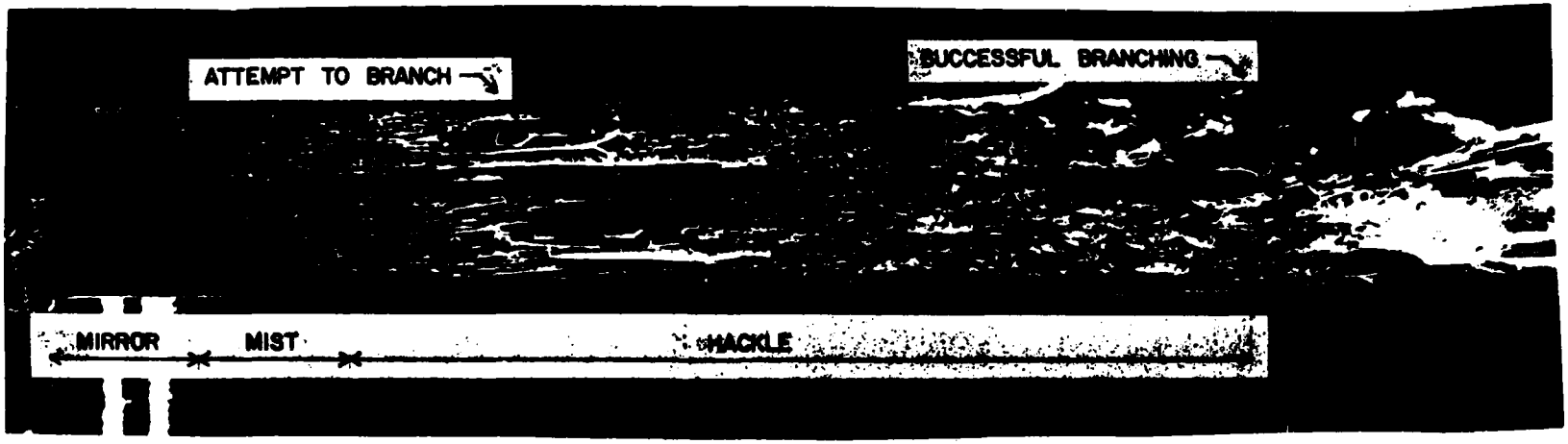

FIGURE 11. FRACTURE SURFACE SHOWING CONTINUOUS CHANGE IN ROUGHNESS PRIOR TO BRANCHING.

Part 1 - Government
Administrative and Liaison Activities

Office of Naval Research
Department of the Navy
Arlington, VA 22217
Attn: Code 474 (2)
471
200

Director
Office of Naval Research
Branch Office
666 Summer Street
Boston, MA 02210

Director
Office of Naval Research
Branch Office
536 South Clark Street
Chicago, IL 60605

Director
Office of Naval Research
Branch Office
1030 East Green Street
Pasadena, CA 91106

Naval Research Laboratory (6)
Code 2627
Washington, D.C. 20375

Defense Documentation Center (12)
Cameron Station
Alexandria, Virginia 22314

Navy

Undersea Explosion Research Division
Naval Ship Research and Development
Center
Norfolk Naval Shipyard
Portsmouth, VA 23709
Attn: Dr. E. Palmer, Code 177

Navy (Con't.)

Naval Research Laboratory
Washington, D.C. 20375
Attn: Code 8400
8410
8430
8440
6300
6390
6380

David W. Taylor Naval Ship Research
and Development Center
Annapolis, MD 21402
Attn: Code 2740
28
281

Naval Weapons Center
China Lake, CA 93555
Attn: Code 4062
4520

Commanding Officer
Naval Civil Engineering Laboratory
Code L31
Port Hueneme, CA 93041

Naval Surface Weapons Center
White Oak
Silver Spring, MD 20910
Attn: Code R-10
G-402
K-82

Technical Director
Naval Ocean Systems Center
San Diego, CA 92152

Navy Underwater Sound
Reference Division
Naval Research Laboratory
P.O. Box 8337
Orlando, FL 32806

474:NP:716:lab
78u474-619

Navy (Con't.)

Chief of Naval Operations
Department of the Navy
Washington, D.C. 20350
Attn: Code OP-098

Strategic Systems Project Office
Department of the Navy
Washington, D.C. 20376
Attn: NSP-200

Naval Air Systems Command
Department of the Navy
Washington, D.C. 20361
Attn: Code 5302 (Aerospace and Structures)
604 (Technical Library)
3208 (Structures)

Naval Air Development Center
Warminster, PA 18974
Attn: Aerospace Mechanics
Code 606

U.S. Naval Academy
Engineering Department
Annapolis, MD 21402

Naval Facilities Engineering Command
200 Stovall Street
Alexandria, VA 22332
Attn.: Code 03 (Research & Development)
04B
045
14114 (Technical Library)

Naval Sea Systems Command
Department of the Navy
Washington, D.C. 20362
Attn: Code 03H
312
322
323
05R
32R

Navy (Con't.)

Commander and Director
David W. Taylor Naval Ship
Research and Development Center
Bethesda, MD 20084
Attn: Code 042
17
172
173
174
1800
1844
012.2
1900
1901
1945
1960
1962

Naval Underwater Systems Center
Newport, RI 02840
Attn: Dr. R. Trainor

Naval Surface Weapons Center
Dahlgren Laboratory
Dahlgren, VA 22448
Attn: Code G04
G20

Technical Director
Mare Island Naval Shipyard
Vallejo, CA 94592

U.S. Naval Postgraduate School
Library
Code 0384
Monterey, CA 93940

Webb Institute of Naval Architecture
Attn: Librarian
Crescent Beach Road, Glen Cove
Long Island, NY 11542

Army

Commanding Officer (2)
U.S. Army Research Office
P.O. Box 12211
Research Triangle Park, NC 27709
Attn: Mr. J. J. Murray, CRD-AA-IP

474:NP:716:lab
78u474-619

Army (Con't.)

Watervliet Arsenal
MAGGS Research Center
Watervliet, NY 12189
Attn: Director of Research

U.S. Army Materials and Mechanics
Research Center
Watertown, MA 02172
Attn: Dr. R. Shea, DRXMR-T

U.S. Army Missile Research and
Development Center
Redstone Scientific Information
Center
Chief, Document Section
Redstone Arsenal, AL 35809

Army Research and Development
Center
Fort Belvoir, VA 22060

NASA

National Aeronautics and Space
Administration
Structures Research Division
Langley Research Center
Langley Station
Hampton, VA 23365

National Aeronautics and Space
Administration
Associate Administrator for Advanced
Washington, D.C. 20546

Air Force

Wright-Patterson Air Force Base
Dayton, OH 45433
Attn: AFFDL (FB)
(FBR)
(FBE)
(FBS)
AFML (MBM)

Air Force (Con't.)

Chief Applied Mechanics Group
U.S. Air Force Institute of Technology
Wright-Patterson Air Force Base
Dayton, OH 45433

Chief, Civil Engineering Branch
WLRC, Research Division
Air Force Weapons Laboratory
Kirtland Air Force Base
Albuquerque, NM 87117

Air Force Office of Scientific Research
Bolling Air Force Base
Washington, D.C. 20332
Attn: Mechanics Division

Department of the Air Force
Air University Library
Maxwell Air Force Base
Montgomery, AL 36112

Other Government Activities

Commandant
Chief, Testing and Development Division
U.S. Coast Guard
1300 E Street, NW.
Washington, D.C. 20226

Technical Director
Marine Corps Development
and Education Command
Quantico, VA 22134

Director Defense Research
and Engineering
Technical Library
Room 3C128
The Pentagon
Washington, D.C. 20301

474:NP:716:lab
78u474-619

Other Government Activities (Con't.)

Dr. M. Gaus
National Science Foundation
Environmental Research Division
Washington, D.C. 20550

Library of Congress
Science and Technology Division
Washington, D.C. 20540

Director
Defense Nuclear Agency
Washington, D.C. 20305
Attn: SPSS

Mr. Jerome Persh
Staff Specialist for Materials
and Structures
OUSDR&E, The Pentagon
Room 3D1089
Washington, D.C. 20301

Chief, Airframe and Equipment Branch
FS-120
Office of Flight Standards
Federal Aviation Agency
Washington, D.C. 20553

National Academy of Sciences
National Research Council
Ship Hull Research Committee
2101 Constitution Avenue
Washington, D.C. 20418
Attn: Mr. A. R. Lytle

National Science Foundation
Engineering Mechanics Section
Division of Engineering
Washington, D.C. 20550

Picatinny Arsenal
Plastics Technical Evaluation Center
Attn: Technical Information Section
Dover, NJ 07810

Maritime Administration
Office of Maritime Technology
14th and Constitution Ave., NW.
Washington, D.C. 20230

474:NP:716:lab
78u474-619

PART 2 - Contractors and other Technical
Collaborators

Universities

Dr. J. Tinsley Oden
University of Texas at Austin
345 Engineering Science Building
Austin, TX 78712

Professor Julius Miklowitz
California Institute of Technology
Division of Engineering
and Applied Sciences
Pasadena, CA 91109

Dr. Harold Liebowitz, Dean
School of Engineering and
Applied Science
George Washington University
Washington, D.C. 20052

Professor Eli Sternberg
California Institute of Technology
Division of Engineering and
Applied Sciences
Pasadena, CA 91109

Professor Paul M. Naghdi
University of California
Department of Mechanical Engineering
Berkeley, CA 94720

Professor A. J. Durelli
Oakland University
School of Engineering
Rochester, MO 48063

Professor F. L. DiMaggio
Columbia University
Department of Civil Engineering
New York, NY 10027

Professor Norman Jones
The University of Liverpool
Department of Mechanical Engineering
P.O. Box 147
Brownlow Hill
Liverpool L69 3BX
England

Professor E. J. Skudrzyk
Pennsylvania State University
Applied Research Laboratory
Department of Physics
State College, PA 16801

Universities (Con't.)

Professor J. Klosner
Polytechnic Institute of New York
Department of Mechanical and
Aerospace Engineering
333 Jay Street
Brooklyn, NY 11201

Prof. R. A. Schapery
Texas A&M University
Department of Civil Engineering
College Station, TX 77843

Professor Walter D. Pilkey
University of Virginia
Research Laboratories for the
Engineering Sciences and
Applied Sciences
Charlottesville, VA 22901

Professor K. D. Willmert
Clarkson College of Technology
Department of Mechanical Engineering
Potsdam, NY 13676

Dr. Walter E. Haisler
Texas A&M University
Aerospace Engineering Department
College Station, TX 77843

Dr. Hussein A. Kamel
University of Arizona
Department of Aerospace and
Mechanical Engineering
Tucson, AZ 85721

Dr. S. J. Fenves
Carnegie-Mellon University
Department of Civil Engineering
Schenley Park
Pittsburgh, PA 15213

Dr. Ronald L. Huston
Department of Engineering Analysis
University of Cincinnati
Cincinnati, OH 45221

Universities (Con't.)

Professor G. C. M. Sih
Lehigh University
Institute of Fracture and
Solid Mechanics
Bethlehem, PA 18015

Professor Albert S. Kobayashi
University of Washington
Department of Mechanical Engineering
Seattle, WA 98105

Professor Daniel Frederick
Virginia Polytechnic Institute and
State University
Department of Engineering Mechanics
Blacksburg, VA 24061

Professor A. C. Eringen
Princeton University
Department of Aerospace and
Mechanical Sciences
Princeton, NJ 08540

Professor E. H. Lee
Stanford University
Division of Engineering Mechanics
Stanford, CA 94305

Professor Albert I. King
Wayne State University
Biomechanics Research Center
Detroit, MI 48202

Dr. V. R. Hodgson
Wayne State University
School of Medicine
Detroit, MI 48202

Dean B. A. Boley
Northwestern University
Department of Civil Engineering
Evanston, IL 60201

474:NP:716:lab
78u474-619

Universities (Con't.)

Professor P. G. Hodge, Jr.
University of Minnesota
Department of Aerospace Engineering
and Mechanics
Minneapolis, MN 55455

Dr. D. C. Drucker
University of Illinois
Dean of Engineering
Urbana, IL 61801

Professor N. J. Newmark
University of Illinois
Department of Civil Engineering
Urbana, IL 61803

Professor E. Reissner
University of California, San Diego
Department of Applied Mechanics
La Jolla, CA 92037

Professor William A. Nash
University of Massachusetts
Department of Mechanics and
Aerospace Engineering
Amherst, MA 01002

Professor G. Herrmann
Stanford University
Department of Applied Mechanics
Stanford, CA 94305

Professor J. D. Achenbach
Northwest University
Department of Civil Engineering
Evanston, IL 60201

Professor S. B. Dong
University of California
Department of Mechanics
Los Angeles, CA 90024

Professor Burt Paul
University of Pennsylvania
Towne School of Civil and
Mechanical Engineering
Philadelphia, PA 19104

474:NP:716:lab
78u474-619

Universities (Con't.)

Professor H. W. Liu
Syracuse University
Department of Chemical Engineering
and Metallurgy
Syracuse, NY 13210

Professor S. Bodner
Technion R&D Foundation
Haifa, Israel

Professor Werner Goldsmith
University of California
Department of Mechanical Engineering
Berkeley, CA 94720

Professor R. S. Rivlin
Lehigh University
Center for Application
of Mathematics
Bethlehem, PA 18015

Professor F. A. Cozzarelli
State University of New York at
Buffalo
Division of Interdisciplinary Studies
Karr Parker Engineering Building
Chemistry Road
Buffalo, NY 14214

Professor Joseph L. Rose
Drexel University
Department of Mechanical Engineering
and Mechanics
Philadelphia, PA 19104

Professor B. K. Donaldson
University of Maryland
Aerospace Engineering Department
College Park, MD 20742

Professor Joseph A. Clark
Catholic University of America
Department of Mechanical Engineering
Washington, D.C. 20064

474:NP:716:lab
78u474-619

Universities (Con't.)

Dr. Samuel B. Batdorf
University of California
School of Engineering
and Applied Science
Los Angeles, CA 90024

Professor Isaac Fried
Boston University
Department of Mathematics
Boston, MA 02215

Professor E. Krempl
Rensselaer Polytechnic Institute
Division of Engineering
Engineering Mechanics
Troy, NY 12181

Dr. Jack R. Vinson
University of Delaware
Department of Mechanical and Aerospace
Engineering and the Center for
Composite Materials
Newark, DE 19711

Dr. J. Duffy
Brown University
Division of Engineering
Providence, RI 02912

Dr. J. L. Swedlow
Carnegie-Mellon University
Department of Mechanical Engineering
Pittsburgh, PA 15213

Dr. V. K. Varadan
Ohio State University Research Foundation
Department of Engineering Mechanics
Columbus, OH 43210

Dr. Z. Mashin
University of Pennsylvania
Department of Metallurgy and
Materials Science
College of Engineering and
Applied Science
Philadelphia, PA 19104

Universities (Con't.)

Dr. Jackson C. S. Yang
University of Maryland
Department of Mechanical Engineering
College Park, MD 20742

Professor T. Y. Chang
University of Akron
Department of Civil Engineering
Akron, OH 44325

Professor Charles W. Bert
University of Oklahoma
School of Aerospace, Mechanical,
and Nuclear Engineering
Norman, OK 73019

Professor Satya N. Atluri
Georgia Institute of Technology
School of Engineering and
Mechanics
Atlanta, GA 30332

Professor Graham F. Carey
University of Texas at Austin
Department of Aerospace ENgineering
and Engineering Mechanics
Austin, TX 78712

Dr. S. S. Wang
University of Illinois
Department of Theoretical and
Applied Mechanics
Urbana, IL 61801

Industry and Research Institutes

Dr. Norman Hobbs
Kaman AviDyne
Division of Kaman
Sciences Corporation
Burlington, MA 01803

Argonne National Laboratory
Library Services Department
9700 South Cass Avenue
Argonne, IL 60440

474:NP:716:lab
78u474-619

Industry and Research Institutes (Con't.)

Dr. M. C. Junger
Cambridge Acoustical Associates
54 Rindge Avenue Extension
Cambridge, MA 02140

Dr. V. Godino
General Dynamics Corporation
Electric Boat Division
Groton, CT 06340

Dr. J. E. Greenspon
J. G. Engineering Research Associates
3831 Menlo Drive
Baltimore, MD 21215

Newport News Shipbuilding and
Dry Dock Company
Library
Newport News, VA 23601

Dr. W. P. Bozich
McDonnell Douglas Corporation
5301 Bolsa Avenue
Huntington Beach, CA 92647

Dr. H. N. Abramson
Southwest Research Institute
8500 Culebra Road
San Antonio, TX 78284

Dr. R. C. DeHart
Southwest Research Institute
8500 Culebra Road
San Antonio, TX 78284

Dr. M. L. Baron
Weidlinger Associates
110 East 59th Street
New York, NY 10022

Dr. T. L. Geers
Lockheed Missiles and Space Company
3251 Hanover Street
Palo Alto, CA 94304

Mr. William Caywood
Applied Physics Laboratory

474:NP:716:lab
78u474-619

Industry and Research Institutes (C

Dr. Robert E. Dunham
Pacifica Technology
P.O. Box 148
Del Mar, CA 92014

Dr. M. F. Kanninen
Battelle Columbus Laboratories
505 King Avenue
Columbus, OH 43201

Dr. A. A. Hochrein
Daedalean Associates, Inc.
Springlake Research Road
15110 Frederick Road
Woodbine,, MD 21797

Dr. James W. Jones
Swanson Service Corporation
P.O. Box 5415
Huntington Beach, CA 92646

Dr. Robert E. Nickell
Applied Science and Technology
3344 North Torrey Pines Court
Suite 220
La Jolla, CA 92037

Dr. Kevin Thomas
Westinghouse Electric Corp.
Advanced Reactors Division
P.O. Box 158
Madison, PA 15663

Dr. Bernard Shaffer
Polytechnic Institute of New York
Dept. of Mechanical and Aerospace
Engineering
333 Jay Street
Brooklyn,, NY 11021

Unclassified

SECURITY CLASSIFICATION OF THIS PAGE (When Data Entered)

REPORT DOCUMENTATION PAGE	READ INSTRUCTIONS BEFORE COMPLETING FORM
1. REPORT NUMBER: UWA/DME/TR-82/46 ✓	2. GOVT ACCESSION NO.: AD-A126444
3. RECIPIENT'S CATALOG NUMBER:	
4. TITLE (and Subtitle): Further Studies on Dynamic Crack Branching	5. TYPE OF REPORT & PERIOD COVERED: Technical Report
	6. PERFORMING ORG. REPORT NUMBER: UWA/DME/TR-82/46
7. AUTHOR(s): M. Ramulu, A. S. Kobayashi, B. S.-J. Kang and D. B. Barker	8. CONTRACT OR GRANT NUMBER(s): N00014-76-C-0060
9. PERFORMING ORGANIZATION NAME AND ADDRESS: Department of Mechanical Engineering FU-10 University of Washington Seattle, WA 98195	10. PROGRAM ELEMENT, PROJECT, TASK AREA & WORK UNIT NUMBERS: NR 064-478
11. CONTROLLING OFFICE NAME AND ADDRESS: Office of Naval Research Arlington, VA 22217	12. REPORT DATE: March 1983
	13. NUMBER OF PAGES: 24
14. MONITORING AGENCY NAME & ADDRESS (if different from Controlling Office)	15. SECURITY CLASS. (of this report): Unclassified
	15a. DECLASSIFICATION/DOWNGRADING SCHEDULE

16. DISTRIBUTION STATEMENT (of this Report)

Unlimited

17. DISTRIBUTION STATEMENT (of the abstract entered in Block 20, if different from Report)

18. SUPPLEMENTARY NOTES

19. KEY WORDS (Continue on reverse side if necessary and identify by block number)

Dynamic mixed mode fracture, crack branching, crack curving, fracture angles, dynamic stress intensity factors, dynamic fracture mechanics, non-singular stress, dynamic photoelasticity, fracture surface

20. ABSTRACT (Continue on reverse side if necessary and identify by block number)

The newly derived dynamic crack branching criterion is verified by dynamic photoelastic analysis of dynamic crack branchings in thin polycarbonate, single edged crack tension specimens. Successful crack branching was observed in four specimens and unsuccessful branchings in another. Crack branching consistently occurred when the necessary condition of K_{Ib}= 3.3 MPa$\sqrt{m}$ and the sufficient condition of $r_o=r_c$=0.7 mm were satisfied simultaneously. In the unsuccessful branching test the necessary condition was not satisfied since K_I was always less than K_{Ib}.

DD FORM 1 JAN 73 1473 EDITION OF 1 NOV 65 IS OBSOLETE
S/N 0102-014-6601

Unclassified

SECURITY CLASSIFICATION OF THIS PAGE (When Data Entered)

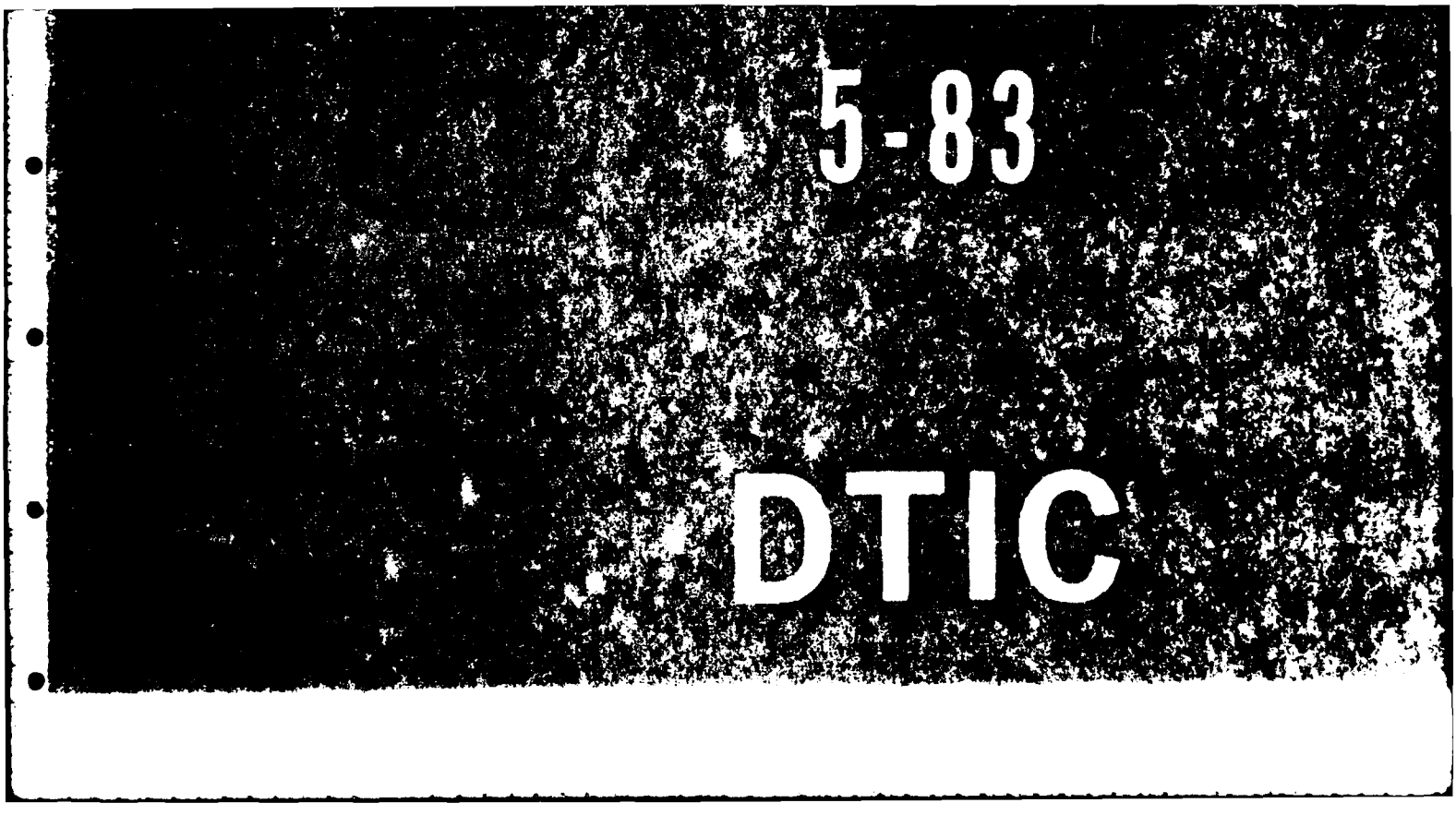
5-83
DTIC